We are IntechOpen, the world's leading publisher of Open Access books Built by scientists, for scientists

4,800
Open access books available

122,000
International authors and editors

135M
Downloads

Our authors are among the

154
Countries delivered to

TOP 1%
most cited scientists

12.2%
Contributors from top 500 universities

CLARIVATE ANALYTICS BOOK CITATION INDEX INDEXED

WEB OF SCIENCE™

Selection of our books indexed in the Book Citation Index in Web of Science™ Core Collection (BKCI)

Interested in publishing with us?
Contact book.department@intechopen.com

Numbers displayed above are based on latest data collected.
For more information visit www.intechopen.com

6

Nonisovalent Alloys for Photovoltaics Applications: Modelling IV-Doped III-V Alloys

Giacomo Giorgi, Hiroki Kawai and Koichi Yamashita
Department of Chemical System Engineering,
School of Engineering, The University of Tokyo
Japan

1. Introduction

In the next thirty years the annual global consumption of energy will rise by more than 50% (Hochbaum & Yang, 2010). Currently most of the energy production comes from the combustion of fossil fuels; nonetheless the deriving CO_2 emissions represent a real risk for the safety of the environment and for human health. Not secondarily, the prompt availability of fossil fuels is extremely influenced by geo-political factors. In the very last decades much attention has been devoted to the development of green renewable energetic sources as possible viable alternative. Owing to its almost ubiquitous availability, solar energy seems to be the most promising way to produce alternative energetic sources. The optimal choice of the materials for the device assembling, according to their prompt availability, in conjunction with recycling spent modules and thinning the semiconductor layers (these two latter are the key-points in reducing the material related sustainability deficits (Fthenakis, 2009)) will help passing from the gigawatt to the terawatt level, that required by the global consumption (Feltrin & Freundlich, 2008). The idea of getting energy from the sun is almost 150 years old. It derives from the discovery of the photovoltaics effect (1839) observed for the first time by the French physicist Edmond Becquerel in an experiment lead with an electrolytic cell made up of two metal electrodes: a weak electrical current was detected by exposing to sunlight a silver coated platinum electrode immersed in electrolyte. From the initial discovery many years have passed until the very first practical application, due to the celebrated Russian physicist Abram Ioffe, consisting in low efficient rectified thallium sulfide cells, has been realized.

The very basic components of a modern solar cell consists in a *p-n* junction, an N-semiconductor, and a P-one, in conjunction with the two electrical contact metal layers that provide the current flow internally and externally to the cell. The main physical quantity that describes a solar cell is the energy *conversion efficiency* (η), defined as the quantity of sunlight converted into electric power. Materials like crystalline Si and GaAs can reach efficiency of about 25%, although efficiencies for most commercially available multicrystalline Si solar cells are below 20%. Solar cells constituted by only one semiconductor material are characterized by a maximum energy efficiency for a bandgap (E_G) between 1.4 and 1.6 eV (Green, 1982).

The other key performance characteristics are represented by the *photocurrent density* (J_{sc}), the *fill factor* (*FF*), and the *open circuit voltage* (V_{oc}), related (also with the incident light power density, P_s) by the general expression:

$$\eta = J_{sc}\, FF\, V_{oc}/P_s \tag{1}$$

Solar cells can operate in a wide range of current (*I*) and voltage (*V*); the *maximum power point* of the cell is defined as the point that maximizes the product between *I* and *V*, in a process that involves the continuous increase of the resistive load on an irradiated cell from *short circuit* to *open circuit* regime. Modern cells can track the power by measuring continously *V* and *I*, equilibrating the load, in order to achieve always the maximum power, regardless of the lighting conditions.

The initial technology of the modern solar cells based on the well-assessed single and multi-crystalline Si cells (the latter cheaper but with reduced quality due to the presence of grain boundaries) has been progressively replaced by the *thin film* based one, the so-called "Second-generation solar cells", usually constituted by GaAs, CuInSe, CIGS (Copper Indium Gallium Selenide), or CdTe, which represent a cheap and simple alternative technology in photovoltaics (PV). A particular mention is deserved by the emerging technology based on the combination of dyes anchored on metal oxides (DSSC, dye sensitized solar cells, (O'Regan & Graetzel, 1991) consisting in porous layers of TiO_2 nanoparticles.

The usage of layered materials with different bandgaps is a desirable procedure for increasing the efficiency of the final PV device. Such assembling procedure results in the splitting of the solar spectrum in several parts. In this way, indeed, photons of different energies are absorbed depending on the used material: the stacking of higher bandgap material on the surface able to absorb high-energy photons with lower-energy photons absorbed by the lower bandgap material beneath is the key step for these *Multi-Junction* (*MJ*), "Third-generation" solar cells, characterized by the reduction of the transmission and that of the thermalization losses of hot carriers. According to the assembling procedure, MJs are *monolithic* or *stacked*. Owing to the requirement of electronic and lattice match of the constituents, the monolithic ones present additional intrinsic difficulties; they are epitaxially grown on Ge substrate and constituted by lattice matched (In,Ga)P and GaAs. The reader may understand the structure of similar devices observing Figures 1-2. In Figure 1, a sketch of (Ga,In)P/(Ga,In)As/Ge is reported, while Figure 2 shows its spectral irradiance of the solar AM1.5 spectrum in conjunction with the parts of the spectrum used. "AM"(Air-Mass) refers to the spectrum of the incident light and corresponds to the shortest, direct optical path length through the Earth atmosphere, that in conjunction with "1.5" represents the standard for the characterization of terrestrial power-generating panels. More precisely, AM is $1/\cos(z)$, where *z* represents the zenith angle. The choice of AM1.5 as standard stems from the fact that it corresponds to $z \sim 43^{o}$, representing the yearly average at mid-latitudes. AM0 is the standard for space cells. In the mechanical stacked MJ the separate connections of top and bottom cells do not mandatorily require current matching, making the combination of bandgaps quite flexible. The only tight requirement is thus the transparent contacts. Anyway, the lattice mismatch may cause crystal dislocations introducing levels in the gap and thus mediating the Shockley-Read-Hall recombination.

Primary role in the rising success of monolithic tandem solar cells must be ascribed to the National Renewable Energy Laboratory (NREL) activity and in particular to the research

conducted by J. M. Olson group (Olson et al., 1985). In details, the initial tandem solar cells based on GaAs and GaInP were made via a vapour phase epitaxy growth process and revealed problems related to the purity of source materials. The initial drawbacks were progressively solved during the nineties and subsequently due to their high efficiency and power-to-mass ratio, systems based on GaInP/GaInAs/Ge have represented and still represent the most reliable choice for communication satellites (Dimroth, 2006). In Figure 3, the calculated conversion efficiency of a triple-junction solar cell as function of the bandgap of the single junctions forming the stacking is reported.

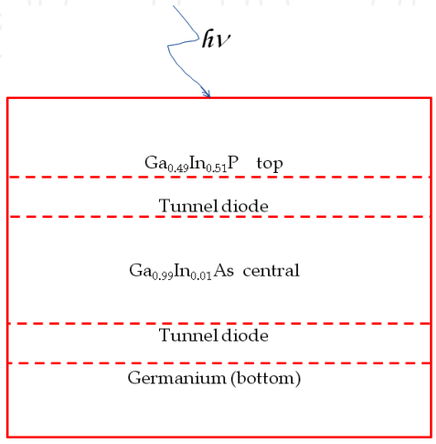

Fig. 1. General structure of a multi-junction solar cell.

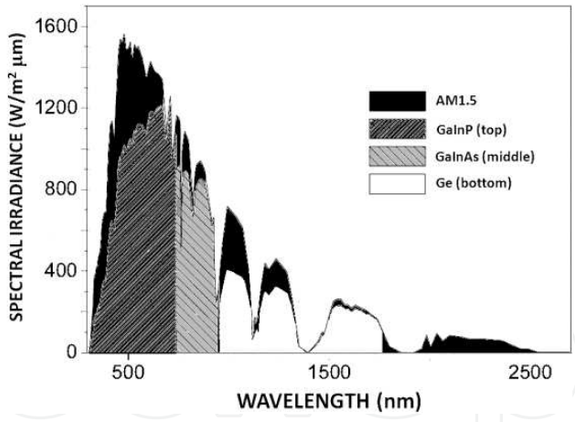

Fig. 2. Spectral irradiance of the solar AM1.5 spectrum with the regions of the spectrum used by a GaInP/GaInAs/Ge 3-junction solar cell.

MJ systems are usually constituted by three different possible substrate: Ge, GaAs, and InP. The introduction of chemical components in the different layers is beneficial (Yamaguchi et al., 2005): Al in the top cell has the property of increasing E_G to values that cover a larger part of the solar spectrum, while few amounts of In reduce the mismatch between layers.
In the context of the Japanese "New Sunshine Project", InGaP/InGaAs/Ge monolithic integrated cells have reached an efficiency of 31.7%, while for the stacked InGaP/GaAs//InGaAs ones an efficiency of 33.3% has been reported (Yamaguchi, 2003), representing at the time of their production the efficiency World Guinness for such cells.

Metamorphic triple-junction $Ga_{0.44}In_{0.56}P/Ga_{0.92}In_{0.08}As/Ge$ terrestrial concentrator solar cells (owing to the macroscopic differences between terrestrial spectrum and the conditions in space, the structure of the solar cell must be adjusted. Therefore, the optimum bandgap combination of materials is not the same) have been recently grown and with the usage of a buffer structure, able to minimize the dislocation formation (King et al., 2007), a record of 40.7% in efficiency has been established in 2007 at 240 suns and at AM1.5D. Even more recently (Guter et al., 2009) a new World Guinness has been established for the metamorphic triple-junction solar cell: an efficiency of 41.1% has been achieved under 454 suns and at same standard conditions: this latter cell combines $Ga_{0.35}In_{0.65}P$ (top cell), $Ga_{0.83}In_{0.17}As$ (middle cell) with a Ge bottom cell. An electrically inactive buffer is used in order to make inactive the formation of threading dislocations that in any case have densities below 10^6 cm^{-2}. Such highly efficient cells are integrated by the usage of a Fresnel lens placed ~10 cm over the cells, ensuring a concentration of the sunlight increased by a factor ranging between 400 and 500.

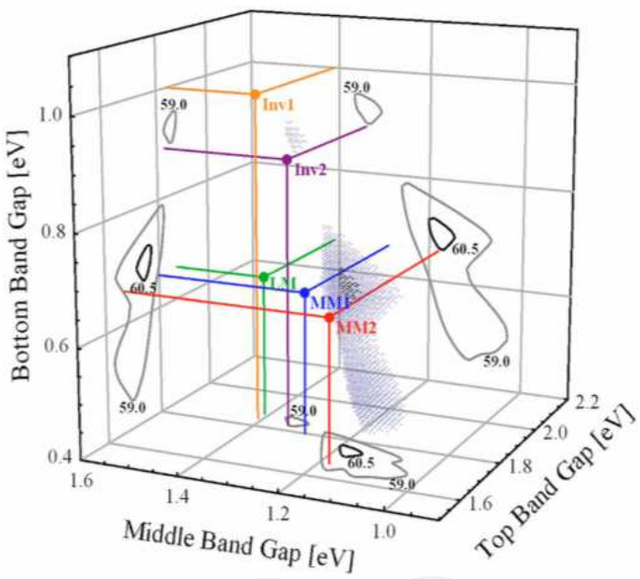

Fig. 3. Detailed balance calculations for the efficiency of different triple-junction solar cell structures under the AM1.5d ASTM G173 – 03 spectrum at 500 kW/m² and 298 K. The black dots represent structures with efficiencies from 60.5% to 61.0% and hence mark the optimal band gap combinations. The gray dots represent structures with an efficiency of 59.0%-60.5% (see contours). Five specific triple junction solar cell structures are also shown. The lattice-matched $Ga_{0.5}In_{0.5}P/Ga_{0.99}In_{0.01}As/Ge$ (LM), two metamorphic GaInP/GaInAs/Ge [(1.8, 1.29, 0.66 eV for MM1) and (1.67, 1.18, 0.66 eV for MM2)], as well as two inverted metamorphic GaInP/GaInAs/GaInAs [(1.83, 1.40, 1.00 eV for Inv1) and (1.83, 1.34, 0.89 eV for Inv2)] devices. [Reprinted figure 3 with permission from: Guter, W.; Schöne, J.; Philipps, S. P.; Steiner, M.; Siefer, G.; Wekkeli, A.; Welser, E.; Oliva, E.; Bett, A. W. & Dimroth, F., *Applied Physics Letters*, Vol. 94, No. 22, pp. 223504-3 ISSN 1077-3118. (2009). Copyright (2011) by the American Institute of Physics].

The continuous research of new materials in PV and the optimization of their performances motivated us to study, in recent years, the electronic and the structural properties of the

alloys formed by IV group elements and the III-V compounds. $(GaAs)_{1-x}(Ge_2)_x$, one of the $(A^{III}B^{V})_{1-x}(C_2^{IV})_x$ nonisovalent alloys, has direct gap ranging between 0.5 and 1.4 eV, ideal for visible-IR light absorption, and lattice constants matching with that of GaAs (5.66 Å (Wang & Ye, 2002)), representing the best candidate in some technologically oriented applications (extra junction of two junction $Ga_{0.52}In_{0.48}P$/GaAs solar cell (Norman et al., 1999)).
In this chapter we review recent results from modelling the structural and electronic properties of such non-isovalent alloys widely utilized in MJ solar cells. The relevance of Density Functional Theory (DFT) and *GW* (*G*: Green function, *W*: screened Coulomb interaction) calculations in this field is discussed and the importance of large modellization in accounting the clusterization phenomena is shown. We also review the basic concepts associated with the stabilizing self-compensation mechanism, both in defective supercells and in alloys.

2. Semiconductor alloys for photovoltaics: The case of $(GaAs)_{1-x}(Ge_2)_x$: A brief overview

The isovalent class of semiconductor alloys represents the most common one (Wei & Zunger, 1989; Shan et al., 1999; Wei et al., 2000; Janotti et al., 2002; Deng et al., 2010) (i.e., IV/IV, (III−V)/(III−V), and (II−VI)/(II−VI)). The alloys belonging to this class are characterized by a reduced band offsets between the constituents (< 1 eV), by a small and composition-independent bowing coefficient, and by a lattice mismatch that is usually below 5% (Zunger, 1999). Differently, the introduction of a low-valent and high-valent element into a III-V compound generates a so called "nonisovalent" alloy (Yim, 1969; Bloom, 1970; Funato et al., 1999; Wang & Zunger, 2003; Osorio et al., 1999; Greene, 1983) (i.e., (III−V)/IV, (III−V)/(II−VI)). High carrier mobilities, an enhanced presence of free electrons and holes according to the growth conditions, and the reduced donor−acceptor charge compensation are the attractive characteristics that make this class matter of deep investigation. In the case of ZnSe−GaAs, Wang *et al.* report only small change in the final alloy bandgap, E_G, as result of the introduction of larger bandgap II−VI dopants into the III−V host, while the opposite (GaAs in ZnSe) causes sharp drops in the bandgap of the alloy (Wang & Zunger, 2003).
In recent years, many other papers have been focused on the class of $(III\text{-}V)_{1-x}(IV_2)_x$ nonisovalent alloys both at theoretical (Holloway, 2002; Newman et al., 1989; Osorio & Froyen, 1993; Ito & Ohno, 1992; Ito & Ohno, 1993; Newman & Jenkins, 1985; Bowen et al., 1983) and experimental (Green & Elthouky, 1981; Barnett et al., 1982; Alferov et al., 1982; Banerjee et al., 1985; Noreika & Francombe, 1974; Baker et al., 1993; Rodriguez et al., 2000; Rodriguez et al., 2001) level. The employment of nonequilibrium grown techniques that incorporate high dopant concentrations in semiconductors has boosted the attention towards this class of alloys. In particular, despite the mutual insolubility of the constituents, the homogeneous single crystal $(GaAs)_{1-x}(Ge_2)_x$ can be synthesized as metastable alloy by sputter deposition technique (Barnett et al., 1982), metal-organic chemical vapor deposition (MOCVD)(Alferov et al., 1982), molecular beam epitaxy (MBE) (Banerjee et al., 1985), and rf magnetron sputtering (Rodriguez et al., 2000; Rodriguez et al., 2001). The direct gap "tailorability" for $(GaAs)_{1-x}(Ge)_{2x}$ alloys is observed in a final large, negative, and asymmetric, *V-shaped*, bowing of the bandgap. Barnett *et al*. (Barnett et al., 1982) report a minimum value of about 0.5 eV at Ge concentration of about 35%: the optical absorption of

homogeneous single-crystal metastable $(GaAs)_{1-x}(Ge_2)_x$ alloys, grown using ultra-high-vacuum ion-beam sputter deposition is there investigated.

Herbert Kroemer, Nobel prize in 2001 for his studies in semiconductor heterostructures used in electronics, clearly states "*…If lattice matching were the only constraint, the Ge-GaAs system would be the ideal heterosystem, as was in fact believed by some of us – including myself – in the early 1960s*". (Kromer, 2001). Then he adds: "*…Covalent bonds between Ge on the one hand and Ga or As on the other are readily formed, but they are what I would like to call valence mismatched, meaning that the number of electrons provided by the atoms is not equal to the canonical number of exactly two electrons per covalent bond*"(Kromer, 2001). And indeed, at equilibrium condition, phase separation between GaAs-rich domains and Ge-rich domains occurs since GaAs and Ge are mutually insoluble due to the formation of what Kroemer calls valence mismatched, otherwise called "bad" bonds (octet-rule violating bonds, i.e., Ga−Ge, As−Ge) (Osorio et al., 1991a). In the ordered GaAs-rich phase, Ga and As preferentially form donor–acceptor pairs, whereas in the Ge-rich phase, they are randomly distributed in the alloy forming a mixture of n-type and p-type semiconductors. The origin of the large bowing is ascribed to this ordered → disordered transition (Newman et al., 1989).

Several other theoretical models have been developed in order to describe such zinc-blend-to-diamond phase transition. They are based on thermodynamic (Newman & Dow, 1983; Newman et al., 1989; Gu et al., 1987; Koiller et al., 1985), percolation (D'yakonov & Raikh, 1982), and stochastic growth approaches (Rodriguez et al., 2000; A Rodriguez at al., 2001; Kim & Stern, 1985; Davis & Holloway, 1987; Holloway & Davis, 1987; Preger et al., 1988; Capaz et al., 1989).

Owing to their intrinsic difficulty in taking into account possible different growth conditions, models based on the percolation method (D'yakonov & Raikh, 1982) predict a critical concentration for the transition at 0.57, quite far from the experimentally reported. In "growth models" the alloy configuration depends on the kinetics of the growth. In such methods no explicit functional minimization is performed (Osorio et al., 1991b) and once that atoms have satisfied the set of growth rules imposed by the model, they are considered as *frozen*, without any further possibility of including the influence of thermal effects. The prediction of the alloy configuration is based on Monte Carlo (MC) models and the atomic position of single layers depends on the epitaxial growth direction. Thus, Long Range Order (LRO) of the final structure depends on the growth direction. Imposed requirement in such models is the "wrong" bond formation (i.e., III−III and V−V) forbiddance. The absence of Sb-Sb bonds in $(GaSb)_{1-x}(Ge_2)_x$ alloy detected via extended X-ray absorption fine structure (EXAFS) experiments (Stern et. al., 1985) confirms the appropriateness of such imposed condition. Kim and Stern have proposed a model specifying in the set of growth rules the equivalent probability for the A^{III} and B^{V} species in the site occupancy, obtaining a critical concentration for the phase transition (x_c) that is 0.26(+0.03/-0.02) on (100) substrate (Kim & Stern, 1985). Such model only considers Short Range Order (SRO), reporting the critical composition below which LRO is present. They also report the x_c dependence by the growth morphology: a planar growth along [100], another, still planar along the [111] direction, and finally a spherical growth model are studied. In this last model the critical Ge concentration is calculated to be smaller than 0.18 (even if this last value is affected by computational limitations that lead to possible inaccuracy). Davis and Holloway have developed another model implemented by MC simulation and analyzed via an analytical approximation. In their model the formation of Ga-Ga and As-As nearest neighbour bonds is forbidden, and

additionally every gallium atom forms a bond with As atom present in excess during the growth process (Davis & Holloway, 1987; Holloway & Davis, 1987). They find a value for $x_c \approx 0.3$ on (100) oriented substrates (Davis & Holloway, 1987). No phase transition is at variance predicted along the <111> direction (Holloway & Davis, 1987), with remnant ZB phase present in all the range of composition. This prediction confirms the experimental findings for $(GaAs)_{1-x}(Ge_2)_x$ obtained via High Resolution X-Ray Diffraction (HRXRD) on several substrate orientations (Rodriguez et al., 2000; Rodriguez et al., 2001).

Rodriguez *et al.* (Rodriguez et al., 2001) compared LRO behaviour with the results of Raman scattering, the experimental procedure for evaluating alloy SRO (Salazar-Hernández, et al. 1999; Olego & Cardona, 1981). In details, they find different LRO for each growth direction. The long range order parameter S for $(GaAs)_{1-x}(Ge_2)_x$ alloys and more in general for the $(III\text{-}V)_{1-x}(IV_2)_x$ is expressed as (Shah et al., 1986):

$$S(x)=2r(x)-1 \tag{2}$$

where r represents the probability that any Ga (As) occupies its site in the lattice. This corresponds to r=1 (0.5) in the case of perfect LRO (disordered crystal). The analysis of Rodriguez of the optical gap and Raman scattering, shows that near-neighbour correlations (SRO) extremely influence the optical properties while, at variance, there is no impact of the substrate orientation and the LRO on the optical properties. Figure 4 reports the mean cluster reciprocal length obtained by Rodriguez by the Monte Carlo simulation for different orientations of the alloy. It is evident from the plot the overall tendency of GaAs clusters in the alloys to reduce their size (fragmentation), increasing the Ge concentration, x. That kinetic models better describe the phase transition than thermodynamic ones is well assessed. The reasons stem from the fact that thermodynamic models do not include the details of the critical composition x_c as a function of kinetic growth, the phase transition critical concentration must be explicitly added as input, and additionally there are no restrictions on the formation of Ga-Ga and As-As bonds. Also a determining role in the nature of the alloy is played by the growth temperature (Banerjee et al., 1985): $(GaAs)_{1-x}Ge_{2x}$ layers epitaxially grown on GaAs (100) substrates at different temperatures analysed by TEM revealed that at T_g = 550 ° C, Ge separated from GaAs into domains of ~100 Å. Differently, single-phase alloys are still detected at T = 430 ° C.

The research described in this chapter has been motivated by the fact that so wide potential applicability of this class of alloys in PV is astonishingly not supported by a deepen knowledge both at Density Functional Theory (DFT) and post-DFT level of their electronic, structural, and optical properties. We thus decided to examine the bowing in $(GaAs)_{1-x}Ge_{2x}$ alloys, searching the microscopic origin of this intriguing and not yet clarified phenomenon. In particular, at first we have theoretically analyzed the properties of four different intermediate structured compounds that range between "pure" GaAs and "pure" Ge (x_{Ge} = 0.25, 0.50 (two samples), 0.75) (Giorgi et al., 2010). Enlarging our models to ones ranging between 8 and 64 atoms, we have investigated the impact of clustering effects and that of the cluster shape on the bandgap bowing (Kawai et al., 2011).

For the alloy electronic properties calculations two of the methods which are reported to give extremely reliable results have been employed: the Quasiparticle Self-consistent *GW* (QS*GW*) approximation approach (van Schilfgaarde et al., 2006) developed by Mark Van Schilfgaarde and his group at Arizona State University and the frequency dependant *GW*

method implemented in the VASP code (VASP) by Shishkin and co-workers. (Shishkin & Kresse, 2006; Shishkin & Kresse, 2007; Fuchs et al., 2007; Shishkin et. al., 2007).

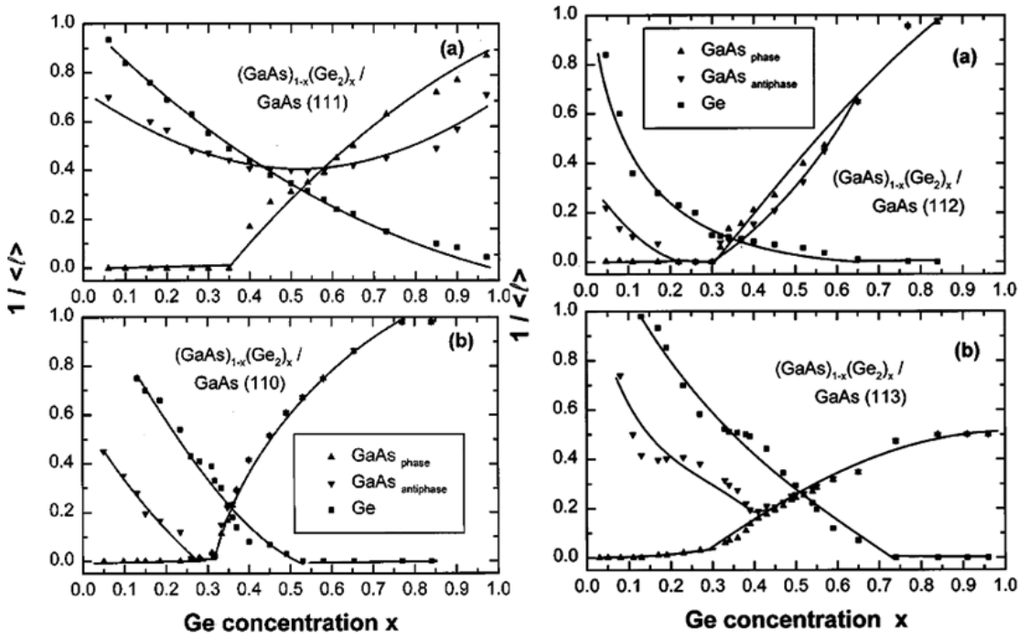

Fig. 4. Left, mean cluster lengths reciprocal (1/<*l*>) from Monte Carlo simulations for (a) (111) and (b) (110) alloys. Full up (down) triangles show the behaviour with Ge concentration for the GaAs phase (antiphase) component. The full squares give the domain size for the Ge component. Right, simulated average cluster reciprocal lengths for (a) (112) and (b) (113) alloys. Full up (down) triangles show the behaviour with Ge concentration for the GaAs phase (antiphase) component. The full squares give the domain size for the Ge component. The lines joining the points are shown for visual aid only. [Reprinted figure 4 with permission from: Rodriguez, A. G.; Navarro-Contreras, H. & and Vidal, M. A., *Physical Review B*, Vol. 63, No. 11, pp. 115328-9, ISSN 1550-235X. (2001). Copyright (2011) by the American Physical Society].

The initial analysis of the 8-atoms cell revealed that the reduction of the bandgap for intermediate x values in $(GaAs)_{1-x}(Ge_2)_x$ alloys takes place with a lattice constant increase and a symmetry reduction with the formation energies linearly related with the number of bad bonds in each model (Giorgi et al., 2010); the subsequent analysis on the shape and the clusterization effects present in these alloys have confirmed at first the main role that SRO plays on asymmetric bandgap behaviour (Rodriguez et al., 2001), further confirming experimental results, like the tendency of large clusters in the alloy to fragment (McGlinn et al., 1988). Large models have been also employed to refine the shape of the asymmetric bowing.

3. Computational details

Using Blöchl's all-electron projector-augmented wave (PAW) method (Blöchl, 1994; Kresse & Joubert, 1999), we performed spin-polarized calculations by using density functional

theory (DFT), within both the local density approximation (LDA) (Perdew & Zunger, 1981; Ceperley & Alder, 1980) and the generalized gradient approximation (GGA) of Perdew and Wang (Perdew, 1991; Perdew et al., 1992) and of Perdew, Burke, and Ernzerhof (PBE, Perdew et al., 1996). In details, *d* electrons in the semicore for both Ga and Ge have been considered. Cutoff energies of 287 and 581 eV were set as the expansion and augmentation charge of the plane wave basis. The force convergence criterion for these models was 0.01 eV/Å.

3.1 The initial case of eight atom unit cells

The initial $(GaAs)_{1-x}Ge_{2x}$ models consisting of 8 atoms were optimized with a 10 x 10 x 10 Γ-centered *k*-points sampling scheme. The reliability of our initial structures has been checked by re-calculating all the total energies with the generalized LMTO method scheme developed by Methfessel *et al.* (Methfessel et al., 1996). We found almost identical results for what regards structural properties and heats of reaction, indicating that the results are well converged. The thermodynamic stability of these alloys was calculated as

$$\Delta E_{form} = E_{alloy} - \{(1-x)E_{GaAs} + xE_{Ge}\} \quad (3)$$

derived from the product-reactant equation:

$$GaAs + 2x\ Ge \rightarrow (GaAs)_{1-x}Ge_{2x} + x\ GaAs \quad (4)$$

Owing to the methodological derived large cancellation of errors, both LDA and GGA are expected to predict reasonable heats of reaction like for that of Eq. (3). At variance with structural properties, optical ones are much less well described, with a well documented underestimation of semiconductor bandgaps. Also dispersion in the conduction band is affected by this DFT shortcoming: for Ge, the LDA gap is negative and Γ_{1c} is lower than L_{1c} in contradiction to experiment. Also the Γ–X dispersion is often strongly affected: in GaAs X_{1c}–Γ_{1c} is about twice the experimental value; underestimations that are generated by the self-interaction error (Perdew & Zunger, 1981) and the discontinuities in the derivatives of exchange-correlation energy (Perdew & Levy, 1983; Sham & Schlüter, 1983).

In the prediction of semiconductor optical properties one of the best method is based on the *GW* approximation of Hedin (Hedin, 1965). This approximation is a perturbation theory around some noninteracting Hamiltonian, H_0. In particular, the quality of this Hamiltonian highly impacts on the quality of the final *GW* result. In conjunction with a "safe" choice of the Hamiltonian, it must be stressed that for reliable results the use of an all-electron method is highly recommended (Gomez-Abal et al., 2008). To satisfy both the requirements, in this initial stage of our calculations, we have adopted here an all-electron method, where not only the eigenfunctions are expanded in an augmented wave scheme, but the screened coulomb interaction *W* and the self-energy Σ = *iGW* are represented in a mixed plane-wave and local-function basis (Kotani & van Schilfgaarde, 2002; Kotani et al., 2007). In addition, all core states are treated at the Hartree-Fock level. In the following we briefly describe the methodology key points.

Usually, in literature the initial Hamiltonian (H_0) for *GW* calculations is an LDA derived guess; thus usual *GW* method may be named $G^{LDA}W^{LDA}$ approximation. Many limitations characterize this $G^{LDA}W^{LDA}$ approaches as reported in previous literature (van Schilfgaarde et al., 2006b). The QuasiParticle Self-Consistent *GW* (QS*GW*) approximation (van

Schilfgaarde et al., 2006a), overcomes most of these limitations. Semiconductor energy band structures are well described with uniform reliability. Discrepancies with experimental semiconductor bandgaps are small and highly systematic and the origin of the error can be explained in terms of ladder diagrams missing in the random phase approximation (RPA) to the polarizability (Shishkin et al., 2007). The RPA results in a systematic tendency for the dielectric constant,ε_∞, to be underestimated. The error is very systematic: ε_∞ is too small by a factor of approximately 0.8, for a wide range of semiconductors and insulators. This fact and also the fact that the static limit of W mainly controls the quasiparticle (QP) excitations, provides a simple and approximate remedy to correct this error: $\Sigma - V_{xc}^{LDA}$ is scaled by 0.8.

3.2 The extension up to 64 atoms

The Short Range Order effects (i.e., those involving shape and the clusterization of GaAs/Ge regions) on asymmetric bandgap behaviour was confirmed in the alloys synthesized by ion-beam sputtering techniques (McGlinn et al., 1988) and *rf* sputtering techniques (Rodriguez et al., 2001). In order to model alloy structures reproducing the SRO effect and deeply understand their effect on the bandgaps, larger supercells (ranging from 8 to 64 atoms) have to be mandatorily investigated to make reliable the comparison with experiments.

In the case of the optimization of larger supercells we made use of similar settings of those of the initial 8-atom cells, being the force convergence criterion still 0.01eV/Å. At variance with the initial case, the number of k-points was still 10×10×10 for models constituted by eight atoms, but in this case we used the Monkhorst-Pack (MP) scheme (Monkhorst & Pack, 1976), checking in this way the possible impact on the final results: our calculations revealed that MP scheme and Γ–centred sampling schemes gave identical results. For the $n_x \times n_y \times n_z$ multiplied supercell models derived from the eight atom unit cell we thus used a $8/n_x \times 8/n_y \times 8/n_z$ k-points sampling scheme. For such larger supercell E_G calculation, we employed a GGA+GW_0 (Fuchs et al., 2007) scheme, using the eigenvalues and wave functions obtained at GGA level as initial guess for GW_0 calculations (eigenvalues only updated, screened potential kept fixed). For the GGA calculations, we used the Perdew-Burke-Ernzerhof (PBE) functional (Perdew et al., 1996). Cut-off energy for response function is 90 eV, and the number of frequency points for dielectric function is 48. The number of unoccupied bands was increased up to 200. A 6×6×6 Γ-centred sampling scheme was used for eight atom models. For the $n_x \times n_y \times n_z$ supercell models of the initial eight atom unit cell we used a Γ-centered $4/n_x \times 4/n_y \times 4/n_z$ k-point sampling scheme.

4. Discussion

4.1 The initial case of eight atom unit cells

A common starting point for both approaches is represented by the calculations at the DFT level of the structural optimized parameters of the two most stable polymorphs of GaAs, zincblende (ZB, group 216, *F-43m*, Z=4) and wurtzite (WZ, group 186, *P63mc*, Z=2) and of Ge in its cubic form (group 227, *Fd-3m*, Z=8) Ge and GaAs, reported in Table 1.

The choice of using LDA in all the subsequent calculations stems from the fact that in this context LDA reproduces structural properties closer to experiment than GGA. Both Ga–As and Ge–Ge bond lengths are 2.43 Å in their most stable polymorph.

ZB–GaAs is constituted by interpenetrating *fcc* sublattices of cations (Ga) and anions (As). The diamond lattice of Ge may be through of as the ZB structure with Ge occupying both

cation and anion sites. In this section we consider 8-atom $(GaAs)_{1-x}Ge_{2x}$ alloy models that vary the Ge composition, including pure GaAs (x=0) to x=0.25 (Ge dimers), x=0.50 (4 Ge atoms), x=0.75 (6 Ge atoms) and finally pure Ge (x=1). Figure 5 reports the structures of the four intermediate alloys. At first we performed an analysis of the Ge dimer in bulk GaAs, at site positions (0.25, 0.25, 0.5) and (0., 0.25, 0.75) , i.e. the alloy model **I.**

	GaAs (ZB) 216, F-43m, Z=4	**GaAs (WZ)** 186, P_{63mc}, Z=2	**Ge (cubic)** 227, *Fd*-3*m*, Z=8
Our analysis, PAW/LDA			
ΔE	**---**	+0.06	----
B	66.14		71.8
Lattice constant (Å)	*a*=5.605	*a*=3.917, *b*=3.886, *c*=6.505	*a*=5.612
Our analysis, PAW/PW91			
ΔE	---	+0.03	**----**
B	79.01		71.0
Lattice constant (Å)	*a*=5.739	*a*=4.040, *c*=6.668	*a*=5.747
Our analysis, PAW/PBE			
ΔE	---	+0.023	----
B	65.94		74.8
Lattice constant (Å)	*a*=5.744	*a*=4.045, *c*=6.670	*a*=5.741
Previous study (GGA)			
B	59.96[a]		55.9[d]
Lattice constant (Å)	*a*=5.74[a],5.722[b]	*a*=3.540, *c*=6.308[c]	*a*=5.78[d]
Previous study (LDA)			
ΔE	---	+0.0120[g]	
B	75.7[e] , 77.1[f]		73.3[d], 79.4[d]
Lattice constant (Å)	*a*=5.654[g],5.53[e] 5.508[f], 5.644[h]	*a*=3.912,*c*=6.441[g] *a*=3.912,*c*=6.407[e]	*a*=5.58[d], 5.53[d]
Experimentally			
ΔE	-----	+0.0117[h]	
B	77.[i]		75.[l]
Lattice constant (Å)	*a*=5.649[i],5.65[j]		*a*=5.678[k] , 5.66[l]

Table 1. The energy difference ($\Delta E_{\text{per unit}}$, eV) between ZB and WZ polymorphs of GaAs, lattice constant, *a*, and bulk moduli *B* (GPa) of GaAs (ZB) and Ge (diamond). ([a]Arabi et al., 2006; [b]A. Wronka, 2006; [c]Bautista-Hernandez et al., 2003;[d] Wang & Ye, 2003;[e]Wang & Ye, 2002; [f]Kalvoda et al.,1997;[g] Yeh et al.,1992; [h]Murayama & Nakayama, 1994;[i]Hellwege & Madelung, 1982; [j]Singh, 1993;[k]CRC, 1997-1998; [l]Levinstein, 1999.)

This model can be considered a highly concentrated molecular substitutional Ge_2 defect in GaAs, for which we predict stability owing to the donor–acceptor self-passivation mechanism (Giorgi & Yamashita, 2011). For a better understanding of this last aspect concerning self-compensation mechanism, we invite the reader to take a look at Section 4.3,

where the stability of Ge substitutional defects (donor, acceptor, and donor-acceptor pairs) in GaAs matrix and its relationship with alloy self-compensation stabilizing mechanism is deeply discussed.

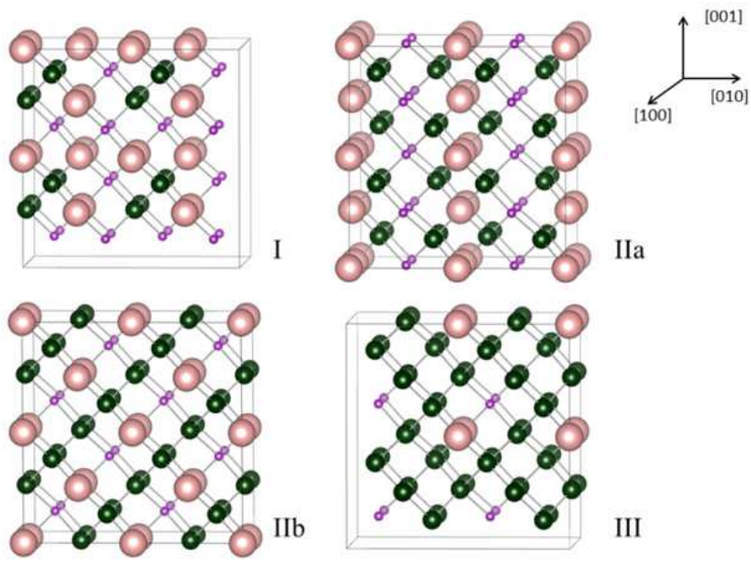

Fig. 5. The four $(GaAs)_{1-x}Ge_{2x}$ alloy models investigated. For visual aid, we here report the 2 x 2 x 2 enlarged cells [Ga, small purple; As, large pink; Ge, intermediate green].

The overall sequence of **I** is a repeated "sandwich-like" structure, ⋯/As/Ge–Ga/Ge–As/Ga/⋯along the (001) direction. The bond lengths are 2.38 (Ga–Ge), 2.42 (Ge–Ge), 2.44 (Ga–As), and 2.47 Å (Ge–As) – only slightly differing from the calculated values in bulk Ge and GaAs (2.43 Å). The small electronegativity variation ($\Delta\chi$) is the explanation of this reduced difference in the bondlength, being Ga-Ge and Ge-As nearly covalent two-center bonds (χ_{Ga}=1.81, χ_{Ge} =2.01, and χ_{As}=2.18).

In the alloy **I** the total number of III-IV and IV-V "bad bonds" (Osorio & Froyen, 1993; Kroemer, 2001; Rodriguez et al., 2001) is 12, or 37.5% of the total. According to the Bader analysis (Henkelmann et al., 2006; Tang et al., 2009; Sanville et al., 2007), in the pure host, the difference in electronegativity is responsible for charge transfer from cation to anion.

In the alloy formation process, the introduction of Ge reduces the ionic character of the GaAs bond, while increasing the ionic character of the Ge–Ge bond. When a Ge dimer is inserted in GaAs, 0.32 electrons are transferred away from Ge_{Ga} site, while Ge_{As} gains 0.21 electrons. The charge deficit on Ga, is reduced from 0.6 electrons in bulk GaAs to 0.47*e* , while the charge excess on As is reduced from 0.6*e* to 0.5*e*. The heat of reaction according to Eq. (3) was 0.55 eV, and the optimized lattice parameter was a=5.621 Å. We have also considered Ge donors (Ge_{Ga}) and acceptors (Ge_{As}) in the pure 8-atom GaAs host cell, separately. The formation energy has been computed according to the Zhang-Northrup formalism (Zhang & Northrup, 1991). In particular, we calculate ΔE to be 1.03 eV for Ge_{Ga} and 0.84 for Ge_{As}. The sum of the single contributions (1.87 eV) is larger than the heat of formation of the dimer, structure **I** (0.55 eV). This is ascribable to the fact that in the model alloy at least one correct bond III-V is formed while in the separate Ge_{Ga} (IV-V) and Ge_{As} (IV-III) cases only bad bonds are formed. The isolated Ge_{Ga} is a donor; the isolated Ge_{As} is an acceptor, thus both of them are unstable in their neutral charged state. We have tested it

in another work (Giorgi & Yamashita, 2011) where we calculated +1 and -1 as the most stable charged state for Ge_{Ga} and Ge_{As} (both isoelectronic with GaAs), for most of the range of the electronic chemical potential. That the stabilization energy 1.32 eV (i.e., 1.87-0.55) is only slightly smaller than the host GaAs bandgap establishes that the self-passivating donor-acceptor mechanism is the stabilizing mechanism of this Ge dimer. As previously stated, for a further and deeper analysis of Ge substitutions in GaAs the reader take a look on Section 4.3.

We considered two alternative structures for the x=0.50 case. In the **IIa** structure Ge atoms are substituted for host atoms at (0.5, 0., 0.5), (0.5, 0.5, 0), (0.75, 0.75, 0.25), and (0.75, 0.25, 0.75). The initial cubic symmetry lowers toward a simple tetragonal one: the optimized lattice parameters were found to be a = 5.590 Å, b = c = 5.643 Å. The 4 intralayer bond lengths were calculated to be Ga–Ge (2.39 Å), Ge–As (2.48 Å), Ge–Ge (2.42 Å), and Ga–As (2.44). Because of the increased amount of Ge, structure **IIa** was less polarized than **I**, as confirmed by the slightly more uniform bond lengths. In **IIa** alloy the number of "bad bonds" is 16 (i.e., 50%) and ΔE rises to 0.72 eV. In the **IIb** structure Ge atoms are substituted for host atoms at (0.25, 0.25, 0.25), (0.25, 0.75, 0.75), (0.75, 0.75, 0.25), and (0.75, 0.25, 0.75). This structure consists of a stack of pure atomic layers, ⋯/Ga/Ge/As/Ge⋯, and thus it contains *only* nearest neighbors of the (Ga-Ge) and (Ge-As) type: thus *all* bonds are "bad bonds" in this **IIb** compound. Bond lengths were calculated to be 2.40 Å and 2.49 Å, respectively, and optimized lattice parameters were a = c = 5.682, b = 5.560 Å. In this structure, ΔE = 1.40 eV, almost double that of **IIa** with identical composition. According to phase transition theory, the symmetry lowering for the two intermediate systems is the fingerprint of an ordered–disordered phase transition. The calculated deviation from the ideal cubic case (c/a=1) is 0.94% and 2.15% for **IIa** and **IIb** models, respectively, confirming energetic instability for the **IIb** alloy. The last model, **III**, [Ge] = 0.75, consists of pure Ge except that Ga at (0., 0. ,0.) and As at (0.25, 0.25, 0.25). The calculated bond lengths were 2.39, 2.43, 2.45, and 2.48 Å for Ga–Ge, Ge–Ge, Ga–As, and Ge–As, respectively. Cubic symmetry is restored: the optimized lattice parameter (a = 5.624 Å) is nearly identical to structure **I**. The formation energy as from Eq.(3) is almost the same as **I** (~0.54 eV). Indeed, **I** and **III** are formally the same model with the same concentration (37.5%) of Ge in GaAs (**I**) and GaAs in Ge (**III**) and the same number of wrong bonds, 12. For sake of comparison between these two cases, we have also calculated the formation energy of a single substituted Ge in the cell.

We have also made a preliminary calculation of the stability of isolated Ga acceptors (Ga_{Ge}) and As donors (As_{Ge}) *vs* that of the substitutional molecular $GaAs_{Ge2}$ in Ge pure host supercell consisting of 64 atoms; for such concentrations (0.0312=1Ge/32GaAs unit and 0.0156=1/64GaAs), the molecular substitutional $GaAs_{Ge2}$ is only stabilized by 0.057eV with respect to the separate couple acceptor-donor. This small stabilization for $GaAs_{Ge2}$ compared to isolated Ga_{Ge} and As_{Ge} confirms the expected similar probability of finding a mixture of *n*-type and *p*-type semiconductors in the "disordered" Ge-rich phase. We have used the most stable polymorph of the elemental compounds (orthorhombic Ga and rhombohedral As) for the chemical potential, μ, of both elements (Mattila & Nieminen, 1996).

Ga-rich ($\mu_{Ga}=\mu_{Ga}^{bulk}$) and As-rich ($\mu_{As}=\mu_{As}^{bulk}$) conditions have been considered, respectively. In the case of the 8-atom cells, the formation energy for Ga_{Ge} and As_{Ge} are 0.26 eV and 0.58 eV, respectively. The model **III** stabilizes the isolated Ga and As substitutions by 0.30 eV, i.e. the ΔE between the alloy and the isolated substitutionals.

At variance with alloy model **I**, the large energy difference (~0.4 eV) between the stabilization energy and the Ge host bandgap (0.67 eV at 300 K (Kittel, 2005)) reveals that other factors, and not only a self-compensating donor-acceptor mechanism, impact on the final stability of this **III** alloy model.
Our calculations reveal an almost exactly linear relationship between the formation energy and the number of bad bonds, as reported in Figure 6. Such relationship is verified at least for systems containing same number of Ge donors (Ge_{Ga}) and Ge acceptors (Ge_{As}).

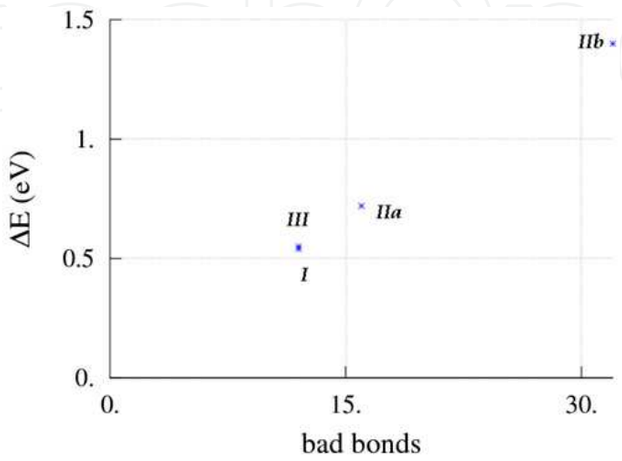

Fig. 6. Heat of formation (ΔE) of the alloy models *vs.* the number of "bad bonds".

This striking result confirms that the electronic structure of these compounds is largely described in terms of independent two center bonds. For stoichiometric compounds, it suggests an elementary model Hamiltonian for the energetics of any alloy with equal numbers of Ge cations and anions. On all the optimized structures QS*GW* calculations have been performed and also for the pure GaAs and Ge 8-atom cells. From Figure 7, where the QS*GW* bandgaps as function of [Ge] are reported, one can see the good reproduction of the asymmetric bowing both at Γ and R points. In particular, QSGW calculated bandgaps for pure GaAs and Ge are 1.66 and 1.04 eV on Γ. **IIb** model (100% of bad bonds), whose bandgap is not reported in Figure 7, has $E_G < 0$ at both the two points, confirming the tight relationship between high concentration of bad bonds and reduced values of the bandgap.

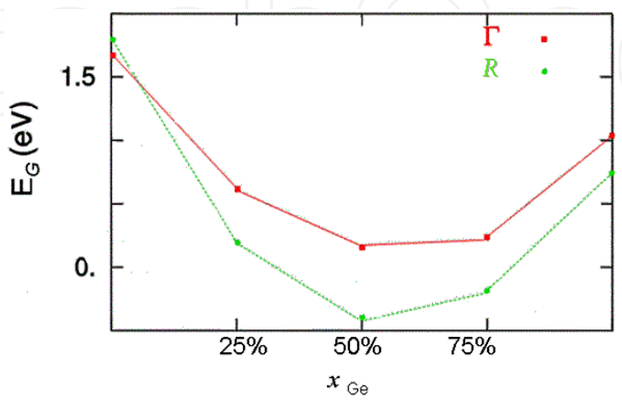

Fig. 7. QS*GW* calculated bowing of the bandgap at Γ and R *vs.* different concentrations of Ge atoms.

4.2 Extended models: The quantitative description of the asymmetric bowing minimum

The subsequent analysis focused on extended alloy models. In particular, we have taken into account here models ranging between 8 and 64 atoms.

Our choice has the two-fold target of confirming the initial results comparing different methodologies for bandgap calculations, and that of investigating the impact that cluster shape and size has in the bandgap itself. It is also supposed that enlarging the size of the models can extremely improve the reproducibility of the asymmetric V-shape of the bandgap bowing. The Special Quasi Random Structures (SQS) methodology (Zunger et al., 1990), developed to incorporate SRO and local lattice distortions in alloy systems, has been widely employed in literature for the description of alloy properties (see Fiorentini & Bernardini, 2001). We stress that the modellization we have here chosen does not lead mandatorily towards a global minimum for each concentration, stemming this choice from the metastable nature of $(GaAs)_{1-x}(Ge_2)_x$ alloys, grown only at nonequilibrium condition (Barnett et al., 1982; Rodriguez et al., 2001; Banerjee et al., 1985; Alferov et al., 1982). The appropriateness of our modellization is confirmed by the high reproducibility of the experimental results we have obtained. McGlinn. (McGlinn et al., 1988) have experimentally found that Ge regions start forming networks as the Ge concentration increased in the range between 0. and 0.3, and at [Ge]=0.3 such networks are connected with each other. This mechanism is accompanied by the GaAs region fragmentation towards size-reduced clusters. Such experimental finding is our driving force in the choice of the enlarged models: we based our study on models reproducing Ge-clusterized alloys at $0< x <0.3$ and GaAs-clusterized alloys at $0.3< x <1$. As stated, experimental results report only the formation of size reduced GaAs clusters for [Ge] > 0.3, thus we decided to compare and discuss local geometry effects and their influence on the bandgap of the two specular models at $x = 0.375$ (such Ge concentration represents the closest one in our models to the experimentally reported concentration, 0.3, where bandgap minimum is found (Barnett et al., 1982)): a Ge-clusterized (**IIIa**) and a GaAs-clusterized (**IIIb**) one. Going back to the discussion regarding our two models at x=0.375, **IIIb** and **IIIa** (whose structure is reported in Figure 8), the former alloy has larger bandgap than the latter, revealing that at low Ge concentration E_G continues decreasing as Ge concentration increases, as long as the alloy geometry is characterized by the presence of Ge clusters embedded in GaAs host, i.e., in a quantum dot-like fashion. Differently, when GaAs turns to clusterize in Ge network, the bandgap stops decreasing. The relationship between the calculated direct gaps along all the range of x is reported in Figure 9, in conjunction with the experimental values.

The close resemblance between our theoretical fitting and the experimental one reveals the extreme suitability of our models in order to reproduce the asymmetric bandgap bowing of $(GaAs)_{1-x}(Ge_2)_x$ alloys: a sharp E_G decreasing at $0< x <0.3$ accompanied by the subsequent smooth increasing at $0.3< x <1$.

Up to now we were able to explain and demonstrate that the bandgap minimum detection is due to the switching of the embedded cluster in the host from a quantum-dot-like fashion (Ge in GaAs) to an *anti*-quantum-dot like fashion (GaAs in Ge). Let us go one step further and let us try to understand the chemical origin of this minimum in the bowing.

As we mentioned, in $(GaAs)_{1-x}(Ge_2)_x$ alloys, the acceptors and donors, when nearest-neighbors, are subjected to stabilizing self-compensation mechanism, while between bad-bond pairs similar mechanism does not occur due to the presence of residual local positive and/or negative charges. However, if such charges can be delocalized, the compensation

can be effective even beyond nearest-neighbor atomic sites. Thus, since the charge distribution on the bad bonds describes the nearest-neighbor atomic chemical environment, it represents a highly valuable analysis to estimate the SRO. In order to investigate the effect of the cluster type *switching* on bad bonds, we analyzed the charge distribution of **IIIa** and **IIIb** models according to the Bader charge analysis scheme (Henkelmann et al., 2006; Sanville et al., 2007; Tang et al., 2009).

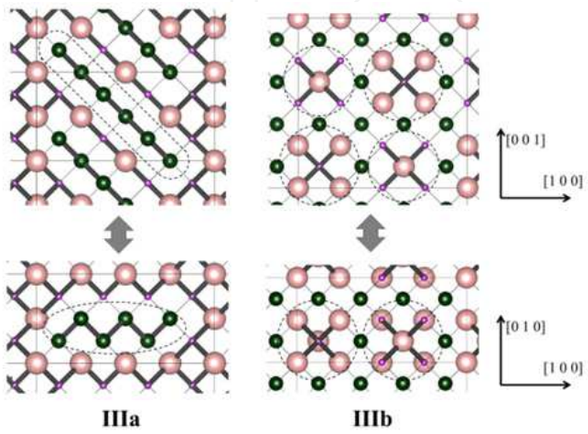

Fig. 8. $(GaAs)_{1-x}(Ge_2)_x$ models at x = 0.375. Left: Top and lateral views of **IIIa** model. Right: Top and lateral views of **IIIb** model. [Pink, large: Ga atoms; purple, small: As atoms; green, intermediate: Ge atoms respectively].

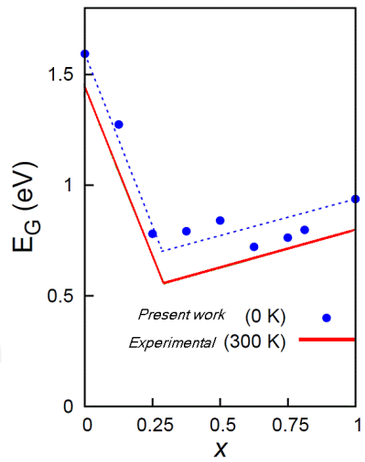

Fig. 9. Our calculated (GGA+GW_0 , (VASP)) and experimental band gap behaviour (Rodriguez et al., 2001) *vs*. Ge concentration (x). Red solid line is fitted to experimental results by two line expressions. Blue points are the calculated values. Blue dotted line is fitted to blue points by two line expressions similar to the red solid one. For x = 0.375, the model **IIIb** bandgap is assumed.

In optimized GaAs, charge on Ga (As) atoms is +0.55e (-0.55e). In model **IIIa**, containing Ge clusters, the charges range between +0.40 and +0.52 for Ga, -0.53 and -0.48 for As, and between -0.29 and +0.32 for Ge, respectively. The charge reduction for Ga and As with

respect to those of pure GaAs are easily explained in terms of electronegativity, χ. $\Delta\chi$ are smaller on bad bonds than on correct Ga-As bonds. Charges on model **IIIb** are +0.30 on Ga, -0.41 on As, and +0.04/+0.08 on Ge, respectively, values extremely reduced if compared with those of **IIIa**. Such charge lowering is explained in terms of number of bad bonds that *single* Ga or As atom forms. In **IIIa**, each Ga and As atom forms 1 or 2 bad bonds. In **IIIb**, on the other hand, each Ga and As atom forms 3 bad bonds. The increase of bad bonds on single Ga and As atom causes partial delocalization of charges, as a consequence of the reduced $\Delta\chi$ between their constituting atoms. This result also impacts the VBM charge density distribution on Γ; indeed, in the **IIIa** model it is localized around the As and Ge, whose electronegativities are larger than Ga (strong charge localization on the formed bad bonds). Thus, similarly to the valence band forward shift ascribed to the charge density localization (non-bonding), the sharp bandgap decrease in the range $0 < [Ge] < 0.3$ is ascribed to the enhancement of the non-bonding character of the VBM. Differently, in **IIIb** the VBM is highly delocalized in the whole crystal. Here, the strong bonding character of VBM stabilizes the system, causing the backward shift of VBM and also the smooth bandgap opening at $0.3 < x < 1$, confirming that SRO effects play the main role in the asymmetric bandgap bowing of this class of alloys.

4.3 On the stability of Ge donor and acceptor defects

In previous sections we have widely taken advantage of the concept of self-passivation. We here focus on this very basic concept of semiconductor physics, showing that regardless the nature of the cell we are considering, alloys or supercells, the self-passivation stabilization mechanism between Ge donor and Ge acceptor pairs is the main stabilizing process in these IV-doped/III-V systems effective also for non nearest neighbor couples. We aim to demonstrate that alloys are super-concentrated defective cells (Giorgi & Yamashita, 2011).The formation energy of the defect is defined as the contribution deriving from the formation energy of the defect in its state of charge, plus the contribution of Ga and As potentials in GaAs, and the potential of the substituting Ge. The thermodynamic stability of the charged substitutional Ge defects is calculated as (Zhang & Northrup, 1991):

$$E_{form} = E_D^{tot} - (n_{Ga} + n_{As})\mu_{GaAs(bulk)}/2 - (n_{Ga}-n_{As})(\mu_{Ga(bulk)} - \mu_{As(bulk)} + \Delta\mu)/2 + q(\mu_e + E_{VBM}) - n_{Ge}\mu_{Ge} \quad (5)$$

where $\Delta\mu$ is the chemical potential difference between bulk GaAs ($\mu_{GaAs(bulk)}$) and bulk Ga ($\mu_{Ga(bulk)}$) and As ($\mu_{As(bulk)}$), respectively, ranges between $\pm\Delta H_{form}$. ΔH_{form} is the heat of formation of bulk GaAs. Beyond the two extreme conditions of $\Delta\mu = \pm\Delta H_{form}$ (Ga-rich and As-rich conditions, respectively) precipitation takes place. μ_e is the electronic chemical potential and E_{VBM} the energy of the top of the valence band (VBM). $n_{Ga(As,\ Ge)}$ is the number of atoms of Ga (As, Ge) in the supercell, while q is its total charge. It is straightforward that this equation is the extension (including the charged case and in the stoichiometric case) of Eq. (3) reported in Section 3.1. Similarly for the alloy case, $\mu_{Ga(As,)}$ is calculated from the orthorhombic (trigonal) polymorph for Ga (As) (Mattila & Nieminen, 1996; Giorgi & Yamashita, 2011). A method based on the combination of the Potential Alignment (PA) for the correction of supercells with a net charge and image charge correction (Lany & Zunger, 2004; Makov & Payne, 1995) has been applied.

To improve the description of the bandgap we employed an LDA + *U* scheme (Dudarev et al., 1998; Giorgi & Yamashita, 2011). VBM and CBM was also corrected and aligned with the LDA +*U* obtained bandgap. The Ge_2 *quasi*-molecule dimer defect best reproduces the high Ge-doping concentration because of the equally probable substitution of one Ga and one As atom, and represents the starting point for our analysis on the self-compensation mechanism in such systems. The neutral state is the most stable along the whole bandgap, as a consequence of the stabilization induced by the mentioned donor–acceptor self-passivating mechanism. The formation energy of the Ge molecular defect is reported in Figure 10.

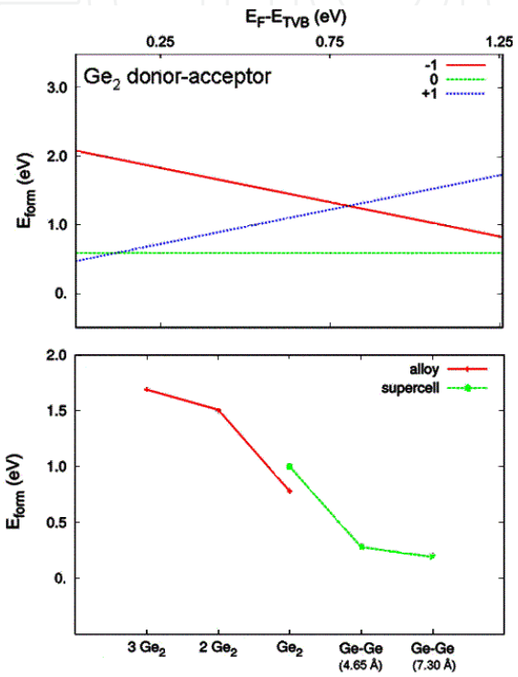

Fig. 10. Top: Formation Energy *vs.* electronic chemical potential of Ge_2 dimer defect. Bottom: Stabilization Energy *vs.* Ge concentration (red) and distance (green) in alloy and defective cells.

We also considered the case of isolated Ge_{Ga} and Ge_{As} ($Ge_{Ga}\cdots Ge_{As}$) pairs in the supercell. Comparison between the ΔE of the three structures (Ge_{2GaAs}, d=2.43 Å, $Ge_{Ga}\cdots Ge_{As}$, d=4.65, 7.30 Å, respectively) reveals the net tendency for Ge to cluster; the first configuration is indeed 0.36 eV more stable than the second and 0.41 eV more stable than the third. This energy difference is due mainly to the formation of one III–IV (Ga–Ge) and one IV–V (Ge–As) bond and the breaking of one IV–IV (Ge–Ge) bond. To evaluate the impact of distance between pairs of substitutionals on the self-compensating mechanism, we have calculated the Ge–Ge pair correlation $J_{(\mathrm{Ge},h\alpha,\mathrm{Ge},h'\beta)}$ as:

$$J_{nn(\mathrm{Ge},h\alpha,\mathrm{Ge},h'\beta)} = [E_{\mathrm{tot}}(\mathrm{GaAs{:}Ge}_{h\alpha}\mathrm{Ge}_{h'\beta}) + E_{\mathrm{tot}}(\mathrm{GaAs})] - [E_{\mathrm{tot}}(\mathrm{GaAs{:}Ge}_{h\alpha}) + E_{\mathrm{tot}}(\mathrm{GaAs{:}Ge}_{h'\beta})] \quad (6)$$

where $E_{\mathrm{tot}}(\mathrm{GaAs{:}Ge}_{h\alpha}\mathrm{Ge}_{h'\beta})$ is the energy for the double Ge-substituted GaAs and $E_{\mathrm{tot}}(\mathrm{GaAs{:}Ge}_{h})$ is that for the single substituted states (h_α and h'_β). The most correlated pair is the *quasi*-molecular Ge_{2GaAs} defect (–1.55 eV), while for the other two cases we calculate a

correlation energy of –1.18 eV for $Ge_{Ga}\cdots Ge_{As}$ at d = 4.65 Å and –1.15 eV for $Ge_{Ga}\cdots Ge_{As}$ at d = 7.30 Å). The SRO included in the difference of the correlation energy between the three distances account for electronic and steric effects. Indeed, the direct formation of Ge–Ge may partly release the stress resulting from substitution of Ga and As in the host. A comparison between the defective supercells and the alloys is here straightforward (see Figure 10, self-compensation mechanism for the two systems).

As in the case of defective supercells also in alloy models, "bad bond" formation and the self-compensation mechanism were considered destabilizing/stabilizing driving forces of the final alloy; we may indeed evaluate the SRO effects on both systems and find a unified trend for alloys and defective supercells. The stabilization energy for the *quasi*-molecular defect is $(E_{Form}(Ge_{Ga}^0) + E_{Form}(Ge_{As}^0)) - E_{Form}(Ge_{2GaAs})$ = 1.60 eV (= $-J_{nn}$, the correlation energy). Effects related to the Ge–Ge direct bond formation give a contribution of 1.01 eV to the total stability (1.60 eV – 0.59 eV). The same contribution for one Ge–Ge bond direct formation in an 8-atom cell alloy was found to be 0.78 eV. Increasing the number of Ge in the alloy results in an increase in the stabilization energy, i.e., 1.51 (= 1.87 – $E_{Form}/2$) eV for two Ge_2, and 1.69 eV (= 1.87 eV – $E_{Form}/3$) for three Ge_2. In the present case, we evaluate how the distance between pairs influences the stabilization energy, or in other words, how self-passivation increases the stability of the overall systems. The stabilization energy for the $Ge_{Ga}\cdots Ge_{As}$ at d = 4.65 Å is 1.18 eV; for $Ge_{Ga}\cdots Ge_{As}$ at d = 7.30 Å the same energy is 1.15 eV. The difference between formation energy and stabilization energy gives the self-passivation contribution, which is 0.28 eV for the former (d = 4.65 Å), 0.19 eV for the latter (d = 7.30 Å); in both cases self-passivation is reduced by the distance. A quantitative trend between the Ge atomic distance and the amount of stabilization due to the self-passivation mechanism is thus computed. Indeed, owing to the reduced difference in terms of atomic radius between the impurity and the host atoms, the stabilizing energy resulting from direct Ge–Ge formation is due purely to electronic factors. This confirms that defective supercells can be considered, regardless of the concentration of the substitutional atoms, as precursors of $(GaAs)_{1-x}Ge_{2x}$ alloys or, similarly, such alloys can be considered as extremely concentrated defective cells.

5. Conclusion

In this chapter we have reviewed the technology behind the Multi-Junction technology in solar cell assembling based on IV-doped III-V alloy showing the importance of Density Functional Theory as a tool for the prediction of the structural and electronic properties of these alloys. After an initial study focusing on eight atom cells, we have extended the analysis to systems constituted by up to 64 atoms. We detected a linear relationship between formation energy and number of bad bonds in the alloys. The relevance of this result stems by the fact that for stoichiometric compounds an elementary model Hamiltonian for the energetics of any alloy with equal numbers of Ge cations and anions as function of the number of bad bonds can be developed. The bandgap bowing for these alloys is confirmed by *GW* calculations. Increasing the cell size we were able to quantitatively reproduce the asymmetric bandgap bowing of $(GaAs)_{1-x}(Ge_2)_x$ alloys. This finding stems from an extremely suitable model choice: moving from previous experimental results, we found that Ge-clusterized alloys at $0 < x < 0.3$ and GaAs-clusterized ones at $0.3 < x < 1$ are the best in reproducing the asymmetric V-shape of the bowing. Turning from Ge-cluster to GaAs-cluster embedding alloys at concentrations close to the experimental reported for the

bandgap minimum is the key-point for the interpretation of this controversial phenomenon. The last part of the Chapter has been dedicated to the discussion of the stability of the Ge donor-acceptor defects in the GaAs supercells. Regardless the distance between Ge pairs in both defective supercells and alloys, the self-passivation mechanism results the driving force of the stabilization of IV-doped III-V systems, being sensitively effective in the former case also for Ge pairs non nearest-neighbors.

6. Acknowledgment

This research was supported by a Grant from KAKENHI (#21245004) and the Global COE Program [Chemical Innovation] from the Ministry of Education, Culture, Sports, Science, and Technology of Japan. GG wants to thanks Dr. G. F. Cerofolini (University of Milano Bicocca) and Dr. A. Korkin (Arizona State University) for the fruitful and stimulating discussions and for a longstanding real friendship.

7. References

Alferov, Zh. I.; Zhingarev, M. Z.; Konnikov, S. G.; Mokan, I. I.; Ulin, V. P.; Umanskii, V. E. & Yavich, B. S. (1982). Preparation and investigation of metastable continuous solid-solutions in the Ge-GaAs system. *Soviet Physics Semiconductors*, Vol. 16, No. 5, pp. 532-537, ISSN 0038-5700.

Arabi, H.; Pourghazi, A.; Ahmadian, F. & Nourbakhsh, Z. (2006). First-principles study of structural and electronic properties of different phases of GaAs. *Physica B: Condensed Matter*, Vol. 373, No. 1, pp. 16-22, ISSN 0921-4526.

Baker, S. H.; Bayliss, S. C.; Gurman, S. J.; Elgun, N.; Bates, J. S. & Davis, E. A. (1993). The effect of varying substrate temperature on the structural and optical properties of sputtered GaAs films. *Journal of Physics: Condensed Matter,* Vol. 5, No. 5, pp. 519-534, ISSN 1361-648X.

Banerjee, I; Chung, D. W. & Kroemer, H. (1985). Properties of $(Ge_2)_x(GaAs)_{1-x}$ alloys grown by molecular beam epitaxy. *Applied Physics Letters*, Vol. 46, No. 5, pp. 494-496., ISSN 1077-3118

Barnett, S. A.; Ray, M.A.; Lastras, A.; Kramer, B.; Greene, J. E.; Raccah, P. M. & Abels, L. L. (1982). Growth and optical properties of single-crystal metastable $(GaAs)_{1-x}Ge_x$ alloys. *Electronic Letters*, Vol. 18, No. 20, pp. 891-892, ISSN 1350-911X.

Bautista-Hernandez, A.; Perez-Arrieta, L.; Pal, U. & Rivas Silva, J. F. (2003). Estudio estructural de los semiconductores AlP, GaAs y AlAs con estructura wurzita. *Revista Mexicana de Fisica*. Vol. 49, No. 001, pp. 9-14, ISSN 0035-001X.

Bernardini, F. & Fiorentini, V. (2001). Nonlinear macroscopic polarization in III-V nitride alloys. *Physical Review B*, Vol. 64, No. 8, pp. 085207-7, ISSN 1550-235X.

Blöchl, P. E. (1994). Projector augmented-wave method. *Physical Review B*, Vol. 50, No. 24, pp. 17953-17979, ISSN 1550-235X.

Bloom, S. J. (1970). Bandgap Variation in Quaternary Alloys. *Journal of Applied Physics*, Vol. 41, No. 4, pp. 1864-1865, ISSN 1089-7550.

Bowen, M. A.; Redfield, A. C.; Froelich, D. V.; Newman, K. E.; Allen, R. E. & Dow, J. D. (1983). Effects of an order–disorder transition on surface deep levels in metastable $(GaAs)_{1-x}Ge_{2x}$. *Journal of Vacuum Science & Technology B: Microelectronics and Nanometer Structures* Vol. 1, No. 3, pp. 747-750, ISSN 1071-1023.

Capaz, R. B.; Preger, G. F. & Koiller, B. (1989). Growth-driven ordering and anisotropy in semiconductor alloys. *Physical Review B*, Vol. 40, No. 12, pp. 8299-8304, ISSN 1550-235X.

Ceperley, D. M. & Alder, B. I. (1980). Ground State of the Electron Gas by a Stochastic Method. *Physical Review Letters*, Vol. 45, No. 7, pp. 566-569, ISSN 1079-7114.

Davis, L. C. & Holloway, H. (1987). Properties of $(GaAs)_{1-x}Ge_{2x}$ and $(GaSb)_{1-x}Ge_{2x}$: Consequences of a stochastic growth process. *Physical Review B*, Vol. 35, No. 6, pp. 2767-2780, ISSN 1550-235X.

Deng, H.-X.; Li, J.; Li, S.-S.; Peng, H.; Xia, J.-B.; Wang, L.-W. & Wei, S.-H. (2010). Band crossing in isovalent semiconductor alloys with large size mismatch: First-principles calculations of the electronic structure of Bi and N incorporated GaAs. *Physical Review B*, Vol. 82, pp.193204-5, ISSN 1550-235X.

Dimroth, F. (2006). High-efficiency solar cells from III-V compound semiconductors. *Physica Status solidi (c)*, Vol. 3, No. 3, pp. 373-379, ISSN 1610-1642.

D'yakonov, M. I. Raikh. M. E. (1982). *Journal Fiuzika i Tekhnika Poluprovodnikov*, Vol. 16, pp. 890. *Soviet Physics Semiconductors,* Vol. 16, pp. 570, ISSN 0038-5700.

Dudarev, S. L.; Botton, G. A.; Savrasov, S. Y.; Humphreys, C. J. & Sutton, A. P. (1998). Electron-energy-loss spectra and the structural stability of nickel oxide: An LSDA+U study. *Physical Review B*, Vol. 57, No. 3, pp. 1505-1509, ISSN 1550-235X.

Feltrin, A. & Freundlich, A. (2008). Material considerations for terawatt level deployment of photovoltaics. *Renewable Energy*, Vol. 33, No. 2, pp. 180-185. ISSN 0960-1481.

Fuchs, F.; Furthmüller, J.; Bechstedt, F.; Shishkin, M. & Kresse, G. (2007). Quasiparticle band structure based on a generalized Kohn-Sham scheme. *Physical Review B,* Vol. 76, No. 11, pp. 115109-8, ISSN 1550-235X.

Fthenakis, V. (2009). Sustainability of photovoltaics: The case for thin-film solar cells. *Renewable and Sustainable Energy Reviews*, Vol. 13, No. 9, pp. 2746-2750, ISSN1364-0321.

Funato, M; Fujita, S. & Fujita, S. (1999). Energy states in ZnSe-GaAs heterovalent quantum structures. *Physical Review B*, Vol. 60, No. 24, pp. 16652-16659, ISSN 1550-235X.

Giorgi, G.; van Schilfgaarde, M.; Korkin, A. & Yamashita, K. (2010). On the Chemical Origin of the Gap Bowing in $(GaAs)_{1-x}Ge_{2x}$ Alloys: A Combined DFT–QS*GW* Study. *Nanoscale Research Letters*, Vol. 5, No.3, pp. 469–477, ISSN 1556-276X.

Giorgi, G. & Yamashita, K. (2011). Amphoteric behavior of Ge in GaAs: an LDA analysis. *Modelling and Simulation in Materials Science and Engineering*. Vol. 19, No. 3, pp. 035001-14, ISSN 1361-651X.

Gomez-Abal, R.; Li, X.; Scheffler, M. & Ambrosch-Draxl, C. (2008). Influence of the Core-Valence Interaction and of the Pseudopotential Approximation on the Electron Self-Energy in Semiconductors, *Physical Review Letters*, Vol. 101, No. 10, pp. 106404-4, ISSN 1079-7114.

Greene, J. E. & Eltoukhy, A. H. (1981). Semiconductor crystal growth by sputter deposition. *Surface and Interface Analysis*. Vol 3, No. 1, pp. 34-54, ISSN 1096-9918.

Greene, J. E. (1983). A review of recent research on the growth and physical properties of single crystal metastable elemental and alloy semiconductors. *Journal of Vacuum Science & Technology B*, Vol. 1, No. 2, pp. 229-237. ISSN n.d.

Green, M. A. (1982). Solar Cells . Prentice-Hall, Englewood Cliffs, NJ,

Gu, B.-L.; Newman, K. E. & Fedders, P. A. (1987). Role of correlations in $(GaSb)_{1-x}Ge_{2x}$ alloys. *Physical Review B,* Vol. 35, No. 17, pp. 9135-9148, ISSN 1550-235X.

Guter, W.; Schöne, J.; Philipps, S. P.; Steiner, M.; Siefer, G.; Wekkeli, A.; Welser, E.; Oliva, E.; Bett, A. W. & Dimroth, F. (2009).Current-matched triple-junction solar cell reaching 41.1% conversion efficiency under concentrated sunlight. *Applied Physics Letters,* Vol. 94, No. 22, pp. 223504-3 ISSN 1077-3118.

Hedin, L. (1965). New Method for Calculating the One-Particle Green's Function with Application to the Electron-Gas Problem. *Physical Review*, Vol. 139, No. 3A, pp. A796-A823, ISSN 1943-2879.

Henkelman, G.; Arnaldsson, A. & Jónsson, H. (2006). A fast and robust algorithm for Bader decomposition of charge density. *Computational Materials Science*, Vol. 36, No. 3, pp. 354-360, ISSN 0927-0256.

Hochbaum, A. I. & Yang, P. (2010). Semiconductor Nanowires for Energy Conversion. Chemical Reviews, Vol. 110, No. 1, pp. 527-546, ISSN 1520-6890.

Holloway, H. (2002). Effect of sample size on simulations and measurements of the phase transition in $(GaAs)_{1-x}Ge_{2x}$ and related alloys. *Physical Review B*, Vol. 66, No. 7, pp. 075131-075136, ISSN 1550-235X.

Holloway, H. & Davis, L. C. (1987). Long-range order in $(GaAs)_{1-x}Ge_{2x}$ and $(GaSb)_{1-x}Ge_{2x}$: Predictions for <111> growth. *Physical Review B*, Vol. 35, No. 8, pp. 3823-3831, ISSN 1550-235X.

Ito, T. & Ohno, T. (1992). Pseudopotential approach to band structure and stability for GaAs/Ge superlattices. *Surface Science*, Vol. 267, No. 1-3, pp. 87-89, ISSN 0039-6028.

Ito, T. & Ohno, T. (1993). Electronic structure and stability of heterovalent superlattices, *Physical Review B*, Vol. 47, No. 24, pp. 16336-16342, ISSN 1550-235X.

Janotti, A.; Wei, S.-H. & Zhang, S. B. (2002). Theoretical study of the effects of isovalent coalloying of Bi and N in GaAs. *Physical Review B*, Vol. 65, pp. 115203-5, ISSN 1550-235X.

Kalvoda, S.; Paulus, B.; Fulde, P. & Stoll, H. (1997). Influence of electron correlations on ground-state properties of III-V semiconductors. *Physical Review B*, Vol. 55, No. 7, pp. 4027-4030, ISSN 1550-235X.

Kawai, H.; Giorgi, G. & Yamashita, K. (2011). Clustering and Octet Rule Violation Impact on Band Gap Bowing: Ab Initio Calculation of the Electronic Properties of $(GaAs)_{1-x}(Ge_2)_x$ Alloys. *Chemistry Letters,* Vol. 40, No. 7, pp. 770-772, ISSN 1348-0715.

Kim, K. & Stern, E. A. (1985). Model for the metastable system of type $(GaAs)_{1-x}(Ge_2)_x$. *Physical Review B,* Vol. 32, No. 2, pp. 1019–1026, ISSN 1550-235X.

King, R. R.; Law, D.C.; Edmondson, K. M.; Fetzer, C. M.; Kinsey, G. S.; Yoon, H.; Sherif, R. A. & Karam, N.H. (2007). 40% efficient metamorphic GaInP/GaInAs/Ge multijunction solar cells. *Applied Physics Letters.* Vol. 90, No. 18 pp. 183516-3, ISSN 1077-3118.

Kittel, C. (2004). Introduction to Solid State Physics, 8th edition, John Wiley & Sons (Ed.) ISBN 0-471-41526-X, New York, USA.

Koiller, B.; Davidovich, M. A. & Osorio, R. (1985). Correlation effects in metastable $(Ga As)_{1-x}$ Ge_{2x} alloys. *Solid State Communications*, Vol. 55, No. 10, pp. 861-864, ISSN 0038-1098.

Kotani, T. & van Schilfgaarde, M. (2002). All-electron GW approximation with the mixed basis expansion based on the full-potential LMTO method. *Solid State Communications*, Vol. 121, No. 9-10, pp. 461-465, ISSN 0038-1098.

Kotani, T.; van Schilfgaarde, M. & Faleev, S. V. (2007). Quasiparticle self-consistent *GW* method: A basis for the independent-particle approximation. *Physical Review B*, Vol. 76, No. 16, pp. 165106-24, ISSN 1550-235X.

Kresse, G. & Joubert, D. (1999). From ultrasoft pseudopotentials to the projector augmented-wave method. *Physical Review B*, Vol. 59, No. 3 pp. 1758-1775, ISSN 1550-235X.

Kroemer, H. (2001). Nobel Lecture: Quasielectric fields and band offsets: teaching electrons new tricks. *Reviews of modern physics*, Vol. 73, No. 3, pp. 783-793, ISSN 1539-0756.

Lany S. & Zunger, A. (2008). Assessment of correction methods for the band-gap problem and for finite-size effects in supercell defect calculations: Case studies for ZnO and GaAs. *Physical Review B*, Vol. 78, No. 23, pp. 235104-25, ISSN 1550-235X.

Makov, G. & Payne M. C. (1995). Periodic boundary conditions in *ab initio* calculations. *Physical Review B*, Vol. 51, No. 7, pp. 4014-4022, ISSN 1550-235X.

Mattila, T. & Nieminen, R. M. (1996). *Ab initio* study of oxygen point defects in GaAs, GaN, and AlN. *Physical Review B,* Vol. 54, No. 23, pp. 16676-16682, ISSN 1550-235X.

McGlinn, T. C.; Klein, M. V.; Romano, L. T. & Greene, J. E. (1988). Raman-scattering and electron-microscopy study of composition-dependent ordering in metastable $(A^{III}B^{V})_{1-x}(C_2^{III})_x$ alloys. *Physical Review B*, Vol. 38, No. 5., pp. 3362-3367, ISSN 1550-235X.

Methfessel, M.; van Schilfgaarde, M. & Casali, R. A. (2000). A full-potential LMTO method based on smooth Hankel functions, In: *Electronic Structure and Physical Properties of Solids: The Uses of the LMTO Method*, Lecture Notes in Physics, H. Dreysse, (Ed.) Vol. 535, pp. 114-147, ISBN 978-3-642-08661-8, Berlin, Germany.

Monkhorst, H. J. & Pack J. D. (1976). Special points for Brillouin-zone integrations. *Physical Review B*, Vol. 13, No. 12, pp. 5188-5192, ISSN 1550-235X.

Murayama, M. & Nakayama, T. (1994). Chemical trend of band offsets at wurtzite/zinc-blende heterocrystalline semiconductor interfaces. *Physical Review B*, Vol. 49, No. 7, pp. 4710-4724, ISSN 1550-235X.

Newman, K. E. & Dow, J. D. (1983). Zinc-blende—diamond order-disorder transition in metastable crystalline $(GaAs)_{1-x}Ge_{2x}$ alloys. *Physical Review B,* Vol. 27, No. 12, pp. 7495-7508, ISSN 1550-235X.

Newman, K. E. & Jenkins, D. W. (1985). Metastable $(III–V)_{1-x}IV_{2x}$ alloys. *Superlattices and Microstructures*, Vol. 1, No. 3, pp. 275-278, ISSN 0749-6036.

Newman, K. E.; Dow, J. D.; Bunker, B.; Abels, L. L.; Raccah, P. M.; Ugur, S.; Xue, D. Z. & Kobayashi, A. (1989). Effects of a zinc-blende–diamond order-disorder transition on the crystal, electronic, and vibrational structures of metastable $(GaAs)_{1-x}(Ge_2)_x$ alloys. *Physical Review B*, Vol. 39, No. 1, 657-662, ISSN 1550-235X.

Noreika, A. J. & Francombe, M. H. (1974). Preparation of nonequilibrium solid solutions of $(GaAs)_{1-x}Si_x$. *Journal of Applied Physics*, Vol. 45, No. 8, 3690-3691, ISSN 1089-7550.

Norman, A.G.; Olson, J. M.; Geisz, J. F.; Moutinho, H. R.; Mason, A.; Al-Jassim, M. M. & Vernon, S. M. (1999). Ge-related faceting and segregation during the growth of metastable $(GaAs)_{1-x}(Ge_2)_x$ alloy layers by metal–organic vapor-phase epitaxy. *Applied Physics Letters*, Vol. 74, No.10, pp.1382-1384, ISSN 1077-3118.

Olego D. & Cardona, M. (1981). Raman scattering by coupled LO-phonon—plasmon modes and forbidden TO-phonon Raman scattering in heavily doped *p*-type GaAs. *Physical Review B*, Vol. 24, No. 12, pp. 7217-7232, ISSN 1550-235X.

Olson, J.M.; Jessert, T.; Al-Jassim, M. M. (1985). GaInP/GaAs: a current- and lattice-matched tandem cell with a high theoretical efficiency. Proc. 18th IEEE Photovoltaic Specialists Conference, Las Vegas, Nevada, 1985, pp. 552-555.

O'Regan, B. & Graetzel, M. (1991). A low-cost, high-efficiency solar cell based on dye-sensitized colloidal TiO_2 films. *Nature.*Vol. 353, pp.737-740, ISSN 0028-0836.

Osório, R.; Froyen, S. & Zunger, A. (1991a). Structural phase transition in $(GaAs)_{1-x}Ge_{2x}$ and $(GaP)_{1-x}Si_{2x}$ alloys: Test of the bulk thermodynamic description. *Physical Review B*, Vol. 43, No. 17, pp. 14055-14072, ISSN 1550-235X.

Osório, R.; Froyen, S. & Zunger, A. (1991b). Superlattice energetics and alloy thermodynamics of GaAs/Ge. *Solid State Communications*, Vol. 78, No. 4, pp. 249-255, ISSN 0038-1098.

Osório, R. & Froyen, S. (1993). Interaction parameters and a quenched-disorder phase diagram for $(GaAs)_{1-x}Ge_{2x}$ alloys. *Physical Review B*, Vol. 47, No. 4, pp. 1889-1897, ISSN 1550-235X.

Perdew, J. P. & Zunger, A. (1981). Self-interaction correction to density-functional approximations for many-electron systems. *Physical Review B*, Vol. 23, No. 10, pp. 5048-5079, ISSN 1550-235X.

Perdew, J. P. & Levy, M. (1983). Physical Content of the Exact Kohn-Sham Orbital Energies: Band Gaps and Derivative Discontinuities. *Physical Review Letters*, Vol. 51, No. 20, pp. 1884-1887, ISSN 1079-7114.

Perdew, J. P. (1991). Electronic Structure of Solids 91, (Akademie Verlag, Berlin 1991). pp.11

Perdew, J. P.; Chevary, J. A.; Vosko, S. H.; Jackson, K. A.; Pederson, M. R.; Singh, D. J. & Fiolhais, C. (1992). Atoms, molecules, solids, and surfaces: Applications of the generalized gradient approximation for exchange and correlation. *Physical Review B*, Vol. 46, No. 11, pp. 6671-6687, ISSN 1550-235X.

Perdew, J. P.; Burke, K. & Ernzerhof, M. (1996). Generalized Gradient Approximation Made Simple. *Physics Review Letters*, Vol. 77, Vol. 18, pp. 3865-3868, ISSN 1079-7114.

Preger, G. F.; Chaves, C. M. & Koiller, B. (1988). Epitaxial growth of metastable semiconductor alloys: A novel simulation. *Physical Review B*, Vol. 38, No. 18, pp. 13447-13450, ISSN 1550-235X.

Rodriguez, A. G., H. Navarro-Contreras, H. & Vidal, M. A. (2000). Long-range order–disorder transition in $(GaAs)_{1-x}(Ge_2)_x$ grown on GaAs(001) and GaAs(111). *Microelectronic Journal*, Vol. 31, No. 6, pp. 439-441; Influence of growth direction on order–disorder transition in $(GaAs)_{1-x}(Ge)_{2x}$ semiconductor alloys. *Applied Physics Letters*, Vol. 77, No. 16, pp. 2497-2499, ISSN 1077-3118.

Rodriguez, A. G.; Navarro-Contreras, H. & Vidal, M. A. (2001). Physical properties of $(GaAs)_{1-x}(Ge_2)_x$: Influence of growth direction. *Physical Review B*, Vol. 63, No. 11, pp. 115328-9, ISSN 1550-235X.

Salazar-Hernández, B.; Vidal, M. A.; Constantino, M. E. & Navarro-Contreras, H. (1999) Observation of zinc-blende to diamond transition in metastable $(GaAs)_{1-x}(Ge_2)_x$ alloys by Raman scattering. *Solid State Communications*, Vol. 109, No. 5, pp. 295-300, ISSN 0038-1098.

Sanville, E.; Kenny, S. D.; Smith, R. & Henkelman, G. (2007). Improved grid-based Algorithm for Bader charge allocation. *Journal of Computational Chemistry*. Vol 28, No. 5, pp. 899-908, ISSN 1096-987X.

Shah, S. I.; Kramer, B.; Barnett, S. A. & Greene, J. E. (1986). Direct evidence for an order/disorder phase transition at $x \approx 0.3$ in single-crystal metastable $(GaSb)_{(1-x)}(Ge_2)_x$ alloys: High-resolution x-ray diffraction measurements. *Journal of Applied Physics*, Vol. 59, No. 5, pp. 1482-1487, ISSN 1089-7550.

Sham, L. J. & Schlüter, M. (1983). Density-Functional Theory of the Energy Gap. *Physical Review Letters*, Vol. 51, No. 20, pp. 1888-1891, ISSN 1079-7114.

Shan, W.; Walukiewicz, W.; Ager III, J. W.; Haller, E. E.; Geisz, J. F.; Friedmann, D. J.; Olson, J. M. & Kurtz, (1999). Band Anticrossing in GaInNAs Alloys. *Physical Review Letters*, Vol. 82, No.6, pp. 1221-1224, ISSN 1079-7114.

Shishkin, M. & Kresse, G. (2006). Implementation and performance of frequency dependent GW method within PAW framework. *Physical Review B,* Vol. 74, No. 3, pp. 035101-13, ISSN 1550-235X.

Shishkin, M. & Kresse, G. (2007). Self-consistent *GW* calculations for semiconductors and insulators. *Physical Review B,* Vol. 75, No. 23, pp. 235102-9, ISSN 1550-235X.

Shishkin, M.; Marsman, M. & Kresse, G. (2007). Accurate Quasiparticle Spectra from Self-Consistent *GW* Calculations with Vertex Corrections. *Physical Review Letters*, Vol. 99, No. 24, pp. 246403-4, ISSN 1079-7114.

Stern, E. A.; Ellis, F.; Kim, K.; Romano, L.; Shah, S. I. & Greene, J. E. (1985). Nonunique structure of metastable $(GaSb)_{1-x}(Ge_2)_x$ alloys. *Physical Review Letters*, Vol. 54, No. 9, 905-908, ISSN 1079-7114.

Tang, W.; Sanville, E. & Henkelman, G. (2009). A grid-based Bader analysis algorithm without lattice bias. *Journal of Physics: Condensed Matter*. Vol. 21, No. 8, 084204-7, ISSN 1361-648X.

van Schilfgaarde, M.; Kotani, T. & Faleev, S. V. (2006a). Quasiparticle Self-Consistent *GW* Theory, *Physical Review Letters*, Vol.96, No. 22, pp. 226402-4, ISSN 1079-7114.

van Schilfgaarde, M.; Kotani, T. & Faleev, S. V. (2006b). Adequacy of approximations in GW theory. *Physical Review B*, Vol. 74, No. 24, pp. 245125-16, ISSN 1550-235X.

VASP, Vienna Ab-initio Simulation Package.

Wang, S. Q. & Ye, H. Q. (2002). A plane-wave pseudopotential study on III–V zinc- blende and wurtzite semiconductors under pressure. *Journal of Physics: Condensed Matter*, Vol. 14, No. 41, pp. 9579-9587, ISSN 1361-648X.

Wang, S. Q. & Ye, H. Q. (2003). *Ab initio* elastic constants for the lonsdaleite phases of C, Si and Ge. *Journal of Physics: Condensed Matter*, Vol. 15, No. 30, pp. L197-L202, ISSN 1361-648X.

Wang, L. G. & Zunger, A. (2003). Dilute non-isovalent (II-VI)-(III-V) semiconductor alloys: Monodoping, codoping, and cluster doping in ZnSe-GaAs. *Physical Review B*, Vol. 68, pp. 125211-8, ISSN 1550-235X.

Wei, S.-H. & Zunger, T. (1989). Band gaps and spin-orbit splitting of ordered and disordered $Al_xGa_{1-x}As$ and $GaAs_xSb_{1-x}$ alloys. *Physical Review B*, Vol. 39, No.5, pp. 3279-3304, ISSN 1550-235X.

Wei, S.-H.; Zhang, S. B. & Zunger, T. (2000). First-principles calculation of band offsets, optical bowings, and defects in CdS, CdSe, CdTe, and their alloys. *Journal of Applied Physics*, Vol. 87, No.3, pp. 1304-1311, ISSN 1089-7550.

Wronka, A. (2006). First principles calculations of zinc blende superlattices with ferromagnetic dopants. *Materials Science-Poland*, Vol. 24, No.3, pp. 726-730, ISSN 0137–1339.

Yamaguchi, M. (2003). III–V compound multi-junction solar cells: present and future. *Solar Energy Materials & Solar Cells,* Vol. 75, No. 1-2, pp. 261-269, ISSN 0927-0248.

Yamaguchi, M; Takamoto, T; Araki, K; Ekins-daukes, N (2005). Multi-junction III–V solar cells: current status and future potential. *Solar Energy*, Vol. 79, No. 1, pp. 78-85, ISSN: 0038-092X.

Yeh, C. Y.; Lu, Z. W.; Froyen, S.; Zunger, A. (1992). Zinc-blende–wurtzite polytypism in semiconductors. *Physical Review B*, Vol. 46, No. 16, pp. 10086-10097, ISSN 1550-235X.

Yim, W.M. (1969) Solid Solutions in the Pseudobinary (III-V)-(II-VI) Systems and Their Optical Energy Gaps. *Journal of Applied Physics*, Vol. 40, No.6, pp. 2617-2623, ISSN 1089-7550.

Zhang, S. & Northrup, J. (1991). Chemical potential dependence of defect formation energies in GaAs: Application to Ga self-diffusion. *Physical Review Letters*, Vol. 67, No. 17, pp. 2339-2342, ISSN 1079-7114.

Zunger, A.; Wei, S.-H.; Ferreira J. L. G. & Bernard, J. (1990). Special quasirandom structures. *Physical Review Letters*. Vol. 65, No. 3, pp. 353-356, ISSN 1079-7114.

Zunger, A. (1999). Anomalous Behavior of the Nitride Alloys. *Physica Status Solidi (b)*, Vol. 216, No. 1, pp.117-123, ISSN 1521-3951.

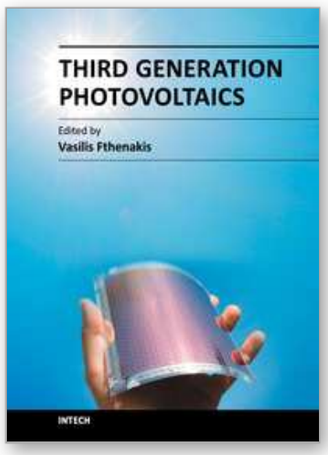

Third Generation Photovoltaics

Edited by Dr. Vasilis Fthenakis

ISBN 978-953-51-0304-2
Hard cover, 232 pages
Publisher InTech
Published online 16, March, 2012
Published in print edition March, 2012

Photovoltaics have started replacing fossil fuels as major energy generation roadmaps, targeting higher efficiencies and/or lower costs are aggressively pursued to bring PV to cost parity with grid electricity. Third generation PV technologies may overcome the fundamental limitations of photon to electron conversion in single-junction devices and, thus, improve both their efficiency and cost. This book presents notable advances in these technologies, namely organic cells and nanostructures, dye-sensitized cells and multijunction III/V cells. The following topics are addressed: Solar spectrum conversion for photovoltaics using nanoparticles; multiscale modeling of heterojunctions in organic PV; technologies and manufacturing of OPV; life cycle assessment of OPV; new materials and architectures for dye-sensitized solar cells; advances of concentrating PV; modeling doped III/V alloys; polymeric films for lowering the cost of PV, and field performance factors. A panel of acclaimed PV professionals contributed these topics, compiling the state of knowledge for advancing this new generation of PV.

How to reference

In order to correctly reference this scholarly work, feel free to copy and paste the following:

Giacomo Giorgi, Hiroki Kawai and Koichi Yamashita (2012). Nonisovalent Alloys for Photovoltaics Applications: Modelling IV-Doped III-V Alloys, Third Generation Photovoltaics, Dr. Vasilis Fthenakis (Ed.), ISBN: 978-953-51-0304-2, InTech, Available from: http://www.intechopen.com/books/third-generation-photovoltaics/nonisovalent-alloys-for-photovoltaics-applications-optical-and-electronic-properties-of-iv-doped-iii

INTECH
open science | open minds

InTech Europe
University Campus STeP Ri
Slavka Krautzeka 83/A
51000 Rijeka, Croatia
Phone: +385 (51) 770 447
Fax: +385 (51) 686 166
www.intechopen.com

InTech China
Unit 405, Office Block, Hotel Equatorial Shanghai
No.65, Yan An Road (West), Shanghai, 200040, China
中国上海市延安西路65号上海国际贵都大饭店办公楼405单元
Phone: +86-21-62489820
Fax: +86-21-62489821

IntechOpen